

Feature Extraction for Outdoor Mobile Robot Navigation Based on a Modified Gauss-Newton Optimization Approach

Sen Zhang Lihua Xie Martin David Adams

*School of Electrical and Electronic Engineering, BLK S2
Nanyang Technological University, Singapore 639798*

Abstract

This paper discusses the problem of feature detection for semi-structured outdoor environments such as campuses and parks using laser range sensors. In these environments, commonly encountered natural features that can be very useful for mobile robot navigation include edges (large discontinuity) and circles (eg, trees, pillars). The term feature is used to denote objects which are “likely” to be detectable when the sensor is moved to new locations. Note that there has been no systematic approach for feature detection in outdoor environments. In this paper, we present an algorithm for feature detection. The algorithm consists of data segmentation and parameter acquisition. A modified Gauss-Newton method is proposed for fitting circular parameters iteratively. Experimental results show that the proposed algorithm is efficient in detecting features for semi-structured outdoor environments and is applicable to real time simultaneous localization and mapping.

Key words: Semi-structured outdoor environments; Feature extraction; Data association; Optimization; Mobile Robot

1 Introduction

Navigation is one of the basic problems for autonomous mobile robots. Its history can be traced back to 4000 years ago. Today, navigation is a well-understood quantitative science, used routinely in maritime and aviation applications [15,2,12]. Given this, the question must be asked as to why robust

Email address: elhxie@ntu.edu.sg (Sen Zhang Lihua Xie Martin David Adams).

and reliable autonomous mobile robot navigation remains such a difficult problem. The core of the problem is the reliable acquisition or extraction of information about navigation beacons from sensor information and the automatic correlation or correspondence of these with some navigation map [11].

Many navigation systems use artificial beacons to realize their navigation task, but the approach may not be realistic in applications such as exploration of jungles or other unknown environments. In this situation, one needs to utilize naturally occurring structure of typical environments to achieve a similar performance. Hence, fast and reliable algorithms capable of extracting features from a large set of noisy data are important in such applications. Some of the early efforts in this direction have focused on extracting line features in an indoor environment based on the information provided by sonar and laser sensors. In [5], a least-squares line fitting technique was applied to extract edges from ultrasonic sensor data. In [18], a recursive line fitting system is used to extract line segments under polar coordinates and an ellipse fitting method is also implemented for data from a laser sensor. In [19], line segments are detected using a regression least-squares parameter estimation method whereas the center and radius of a circle feature are estimated based on the average value of the measurements of the circle from a 2D range scanner. Instead of fitting straight line segments after a full scan has been recorded, Adams presented an on-line edge extraction approach employing a Kalman filter in [3]. Later, based on this method, a two-layer Kalman filter was used to calculate the parameters of a line by an on-line method in [17]. Observe that the aforementioned articles are focused on indoor applications and are mainly concerned with line extraction.

For an outdoor environment, the problem of feature selection and detection is more challenging. In our view, in most typical semi-structured outdoor environments, such as campuses, parks and suburbs, tree trunks and tree-like objects, such as pillars, are relatively stable, regular and naturally occurring features that can provide very useful information for mobile robot navigation. Recently, some research on the use of these kinds of geometrical features has been carried out in [10,20]. Also, [10,4] addressed the problem of extracting tree trunks from laser scan data where the centre and radius of a circle are estimated by averaging the measurements. This method can be susceptible to outliers which can significantly affect the accuracy of the center and radius estimates. Other relevant works include graphics for circle detection, see, for example, Philippe Dosch *et. al* [9] where an arc detection algorithm for vision data is presented. The approach is based on recursive splitting to segment a curve into a set of arcs and segments via least-squares minimization. Also Doris proposed a vector-based arc segmentation in [8]. There are however some unknown parameters are required and the computational requirement of these algorithms is high although they give a robust solution.

In this paper, we shall address the problem of extracting edge and circle features for semi-structured outdoor mobile robot navigation. We classify features into edges, circles and random clutter and propose an approach for their extraction. First, a model based data segmentation method is applied which divides the collected data into groups that are possibly associated with different features of the environment. The extended Kalman filter or other filtering techniques can be applied for segmentation. Edges are also detected during segmentation. We then give a procedure to identify the type of features with which a given group of data is associated. For a circle feature, a modified Gauss-Newton optimization is proposed to obtain estimates of its centre and radius. Several experiments are carried out to demonstrate the feasibility and effectiveness of the proposed feature extraction method. In the experiments, the data association method proposed in [21] is used to enhance the robustness of features. The results show that our method for feature extraction is implementable in real-time and outperforms existing methods such as that in [4].

The structure of the paper is as follows: Section 2 presents our feature extraction algorithm, and section 3 shows the experimental results using the proposed algorithm in several outdoor environments. Conclusions are drawn in Section 4.

2 Feature Extraction Algorithm

We observe that in many semi-structured outdoor environments, planes such as building walls and cylindrical surfaces such as tree trunks or tree-like objects are often encountered. We consider two kinds of features for these semi-structured environments. Observe that in most outdoor environments, trees or tree trunks can be very useful features for mobile robot navigation. In [11,4], the problem of extracting circle features was addressed by averaging their measurements. Here, we shall propose an algorithm which is able to extract edges and tree trunks with a higher accuracy. The essential components of this algorithm include two parts: the first is the segmentation of the scan data and the second is the parameter acquisition.

2.1 Data Segmentation and Edge Detection

Segmentation is a process of aiming to classify a set of scan data into several groups, each of which possibly associates with different structures of the surroundings. The segmentation process is realized through the EKF [3] or other filtering techniques. At each time instant the range estimate is compared to

the range measurement based on their statistics in order to decide if an edge has been detected. When the difference between the measured range and the predicted range is beyond a certain threshold, we consider that an edge has been detected. This can be achieved by using a validation gate during the prediction process with the EKF.

2.1.1 Planar Model

Let us first introduce a mathematical framework for a planar surface. Consider a vertical plane shown in Fig. 1 and the corresponding sensed data points from a perfect 3D line of the sight sensor. Similar to the description in [2,3], we have:

$$d_{i+2} = \frac{d_i d_{i+1}}{2d_i \cos \gamma - d_{i+1}} \quad (1)$$

where γ is the constant angle between successive samples of the sensor as it rotates about its vertical axis. Note that the relationship given in equation (1) is independent of the elevation angle α .

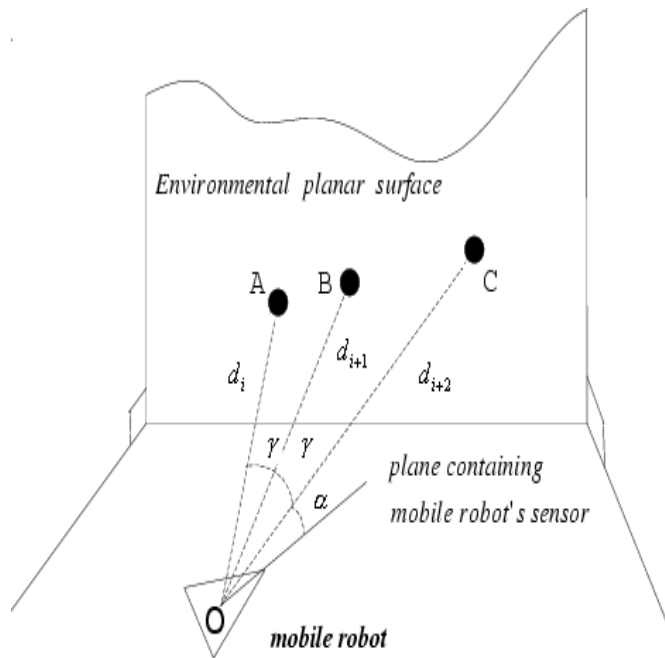


Fig. 1. The relationship between successive range readings when scanning a planar surface

2.1.2 System Model

Equation (1) is clearly a second order difference equation with respect to time. We define $x_1(k+1) = d_{i+2}$ and $x_2(k+1) = x_1(k) = d_{i+1}$, where $x_1(k)$ and $x_2(k)$ are the state variables at time instant k . Therefore equation (1) can be fully defined by the state space equations:

$$\mathbf{x}(k+1) = \mathbf{f}_1(\mathbf{x}(k)) + \mathbf{v}(k) \quad (2)$$

where $\mathbf{x}(k+1) = [x_1(k+1) \ x_2(k+1)]^T$,

$$\mathbf{f}_1(\mathbf{x}(k)) = \begin{bmatrix} \frac{x_1(k)x_2(k)}{(2x_2(k)\cos\gamma - x_1(k))} \\ x_1(k) \end{bmatrix}$$

and $\mathbf{v}(k)$ is the process noise which reflects possible imperfection of the surface. We assume that $\mathbf{v}(k)$ is a white noise process with covariance $\mathbf{Q}(k)$. Clearly, a small covariance $\mathbf{Q}(k)$ implies that the surface is close to perfect. In the experiments in this paper, we set $Q(k) = 10^{-4}\mathbf{I}$. Equation (2) represents a system model which will be used to predict the next range value from the sensor before the actual range measurement is recorded.

Similar to [2], our observation model is:

$$\mathbf{z}(k) = \mathbf{H}_1 \begin{bmatrix} x_1(k) \\ x_2(k) \end{bmatrix} + \mathbf{w}(k) \quad (3)$$

where $\mathbf{H}_1 = [1 \ 0]$ and $\mathbf{w}(k)$ is a zero mean Gaussian noise with a known variance σ_r^2 . The EKF is used to realize the prediction and validation process.

Note that if the degenerate case (almost parallel) is detected, we suggest that these measurements can be rejected.

2.1.3 Extended Kalman Filter and Validation Gate

Based on the above system model, an extended Kalman filter is used to implement the prediction and update. In order to identify if a measurement is associated with a new edge (large discontinuity), a certain criterion needs to be established. The innovation $\nu(k+1)$ and the innovation variance $\mathbf{s}(k+1)$ is used to define:

$$d(k+1) = \nu^T(k+1)\mathbf{s}^{-1}(k+1)\nu(k+1) \quad (4)$$

where $\mathbf{s}(k+1)$ is the observation innovation variance. Note that since ν is a Gaussian random variable, d is a random variable following the χ^2 distribution.

The smaller $d(k + 1)$ is, the higher the probability that the measurement $z(k + 1)$ is obtained from the same planar surface. Thus, a validation gate, δ , is used to decide whether the measurement $z(k + 1)$ is a close enough match to the predicted data point to continue the filter update. If the measurement is such that $d(k + 1) > \delta$, a discontinuity is found. From the χ^2 distribution table, we know that if the observation is from the same planar surface, then $d(k + 1) < 6.63$ with a probability of 0.99. If a small δ is selected, there will be more edges found. Here we set $\delta = 6.63$.

After the data segmentation process, we need to decide if each segment of data is associated with a line or a circle (note that the laser sensor data points only form an arc which is part of a circle, here we call it a circle feature) or clutter. For a line, the average error between the observation and the EKF prediction at each point should be very small. Note that the prediction error (innovation) sequence $\{\nu\}$ of equation (5) follows a Gaussian white noise and its covariance is given by $\mathbf{s}(k)$. Assume that the number of points of the segment is M . Then the sequence $\{\nu\}$ is of the length $M - 2$ (note that the first two points are used to initialize the filter). The average prediction error and its covariance are then given by

$$\bar{\nu} = \frac{\sum_{k=3}^M \nu(k)}{M - 2}, \quad \bar{\mathbf{s}} = \frac{\sum_{k=3}^M \mathbf{s}(k)}{(M - 2)^2} \quad (5)$$

Hence, $P\{|\bar{\nu}| \leq 3\sqrt{\bar{\mathbf{s}}}\} = 0.997$. A threshold for the average prediction error can be chosen as $3\sqrt{\bar{\mathbf{s}}}$. The threshold is used to distinguish a line from a circle or clutter. If the average prediction error is smaller than the threshold, we consider that this segment of data is associated with a line, otherwise, it is associated with a circle or clutter. Note that if a circular shaped clutter is detected as a circle feature after several successive scans, the circular shaped clutter is considered to be the same as a circle feature. If after several successive scans, we can not detect the circle feature that was found in the previous scans, the feature detected should be a circular shape clutter.

For a circle, we need to estimate its parameters such as the center and the radius of the circle so that future measurements of the circle may be used for robot navigation. In the following, the modified Gauss-Newton method [16,6] is applied.

2.2 Parameter Acquisition

A circle can be defined by the equation $(x - x_0)^2 + (y - y_0)^2 = r^2$ where (x_0, y_0) and r are the center and the radius of the circle, respectively. For fitting a circle,

a known data set (x, y) is determined and the circle parameters (x_0, y_0, r) need to be estimated. Assume that we have obtained M measurements (x_m, y_m) , $m = 1, 2, \dots, M$, of the circle. Our objective is to find $p = (x_0, y_0, r)$ that minimizes

$$E(p) = E(x_0, y_0, r) = \sum_{m=1}^M [(x_m - x_0)^2 + (y_m - y_0)^2 - r^2]^2 \quad (6)$$

This is equivalent to performing the least-squares process using the equations

$$g_m(x_0, y_0, r) = (x_m - x_0)^2 + (y_m - y_0)^2 - r^2 = 0, \quad m = 1, 2, \dots, M \quad (7)$$

The equation (7) is not linear about the unknown parameters x_0 , y_0 , and r , therefore it is a nonlinear least-squares problem. We propose to use the modified Gauss-Newton optimization method [16,6] to solve the problem.

Remark 2.1 *Note that the Hough transform is commonly used for parameter acquisition and segmentation [13]. The transform is implemented by quantizing the Hough parameter space into a finite number of accumulator cells. As the algorithm runs, each point is transformed into a discretized curve and the number of intersections of the accumulator cells is counted. However, the problem of how to decide the number of the cells in the parameter space remains unsolved. If the Hough transform is applied for fitting a circle, the parameter space is of three dimensions, which makes the problem more difficult. And with the increased dimension of the parameter space, the Hough transform method becomes more complex and slower. Hence, we use the modified Gauss-Newton method instead of the Hough transform for parameter acquisition.*

In our case the Jacobian matrix for the modified Gauss-Newton algorithm is

$$A = \begin{bmatrix} \frac{\partial g_1}{\partial x_0} & \frac{\partial g_1}{\partial y_0} & \frac{\partial g_1}{\partial r} \\ \frac{\partial g_2}{\partial x_0} & \frac{\partial g_2}{\partial y_0} & \frac{\partial g_2}{\partial r} \\ \vdots & \vdots & \vdots \\ \frac{\partial g_M}{\partial x_0} & \frac{\partial g_M}{\partial y_0} & \frac{\partial g_M}{\partial r} \end{bmatrix} \quad (8)$$

Let $\bar{g} = (g_1 \ g_2 \ \dots \ g_M)^T$ with g_m as defined in (7).

At the k -th step, the modified Gauss-Newton method is applied to search for the solution according to the following equation:

$$(A_k^T A_k + \lambda_k I) \Delta p_k = -A_k^T \bar{g}_k \quad (9)$$

where $\Delta p_k = p_{k+1} - p_k$ and p_k is the estimate of $p = [x_0 \ y_0 \ r]^T$ at the k -th

iteration. We set the initial value $\lambda_0 = 0.01$ (by estimation) and carry out the following iterations for calculating a suboptimal p :

Step 1: Calculate Δp_k using equation (9);

Step 2: Calculate the sum error $E(p_k + \Delta p_k)$ by equation (6);

Step 3: Compare $E(p_k + \Delta p_k)$ with the sum error of last step $E(p_k)$. If $E(p_k + \Delta p_k) > E(p_k)$, increase λ_k by a factor of 10, and go back to Step 1;

Step 4: If $E(p_k + \Delta p_k) < E(p_k)$, decrease λ_k by a factor of 10, update the trial solution, i.e. replace p_k by $p_k + \Delta p_k$ and go back to Step 1 until the algorithm converges.

The convergence condition can be defined by the sum of the squared error and the number of iterations.

Observe that a starting guess for these parameters is required. We use the first three points (x_i, y_i) $i = 1, 2, 3$ and equation (7) to compute an estimated initial value of (x_0, y_0, r) . The more accurate the initial value is, the faster the algorithm converges.

Remark 2.2 *In our algorithm, since each group of data is formed after data segmentation, any measurement outliers have been removed since an outlier produces a large discontinuity in segmentation. On the other hand, in complex outdoor environments, features extracted by the above proposed method may become unstable. These unstable features mean the features that cannot be confirmed (used more than 3 times) during the SLAM process. In order to use these features for navigation, the correspondence between a current feature extracted by the above method and a feature in the map built thus far has to be established. This is the so-called data association problem. In this paper, we apply the data association algorithm proposed in [21] [23] where the problem is formulated as a (0,1) integer programming one and solved by a combined linear programming and iterative heuristic greedy rounding (IHGR) method. The details can be found in [21] [23] and will not be repeated here.*

Remark 2.3 *In the present study we have assumed that there exists no angular uncertainty of the sensor. In practice, however, even though for laser range finders, the angular uncertainty does exist and can be incorporated in the algorithm. This will be considered in the future study.*

3 Experimental Results

The laser sensor used in the following experiments is Sick PLS200. The field of view is 180 degrees in front of the robot and it has a range measuring capability of up to 50 meters. To obtain a 360 degree scan, we use 2 back to back Sick sensors. The range samples are spaced every half a degree, all within the same plane.

In the first experiment, data is collected outdoors as shown in Fig. 2(a) where there are 10 pillars labelled from *a* to *j*, and the surroundings are building walls and low balusters with small shrubs at a long distance. In this figure, the six cross points (+) represent the six positions at which the robot scans the surroundings. The laser scanner is placed on top of a mobile robot at approximately 1.2 meters above the ground. At this level, the sensor can see objects beyond the balusters. In Fig. 2(b), we show real data from one scan of the environment. The robot is located at the origin. Because the distance of some objects is very near to the sensor, the points here are not very regularly distributed, see figure 2(b). Feature extraction has been carried out for all 6 scans. In Figures 3(a) and 4(b), we show the feature extraction results at two different positions.

Fig. 3(a) and Fig. 3(b) show the feature extraction results at position 2 using the proposed method of the last section. Zoomed views of the regions inside the dashed box of Fig. 3(a) are given in Fig. 3(b) where the extracted features can be seen clearly. In these figures, the detected edges are denoted by crosses. Similarly, the feature detection results at position 4 are shown in Figures 4(a) and 4(b).

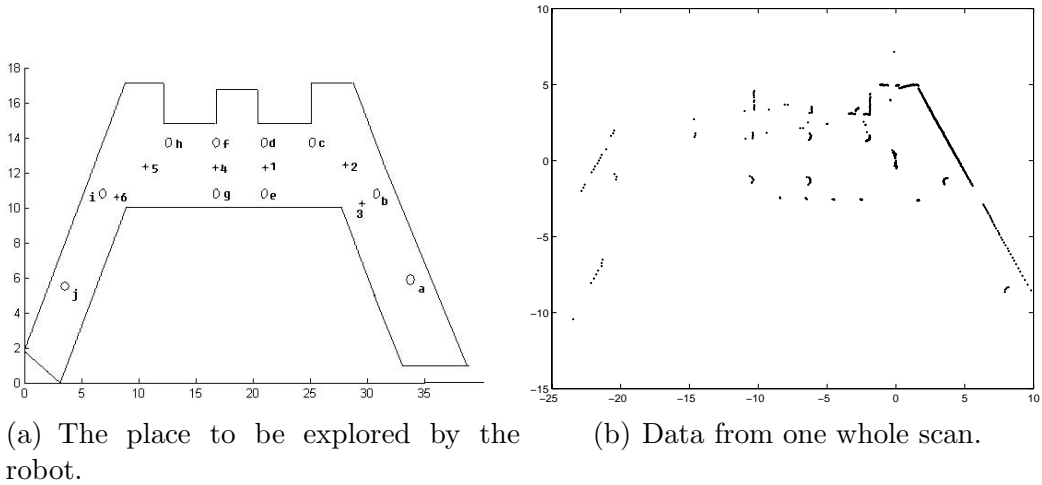
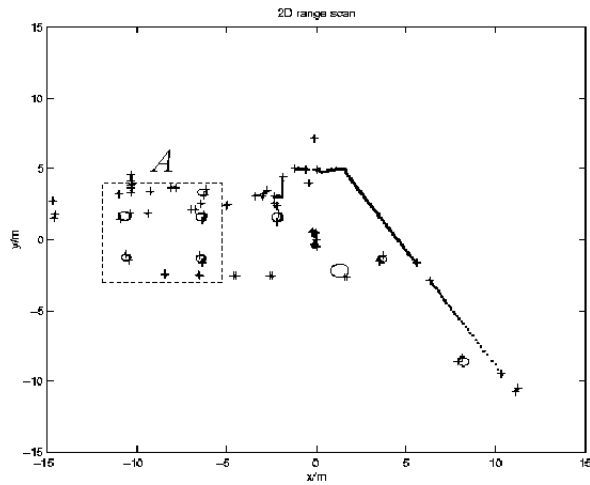
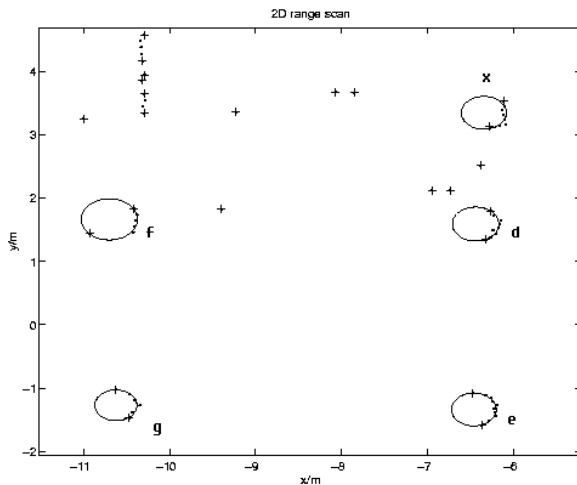


Fig. 2. The environment and the laser scan.

To give an indication of the accuracy of the algorithm, we compare our method with some existing method. In the work by Bailey [4], navigation methods are



(a) Circles and edges extracted from data scanned at position 2 (the normal view).



(b) A zoomed view of the region inside box A in Fig. 3(a).

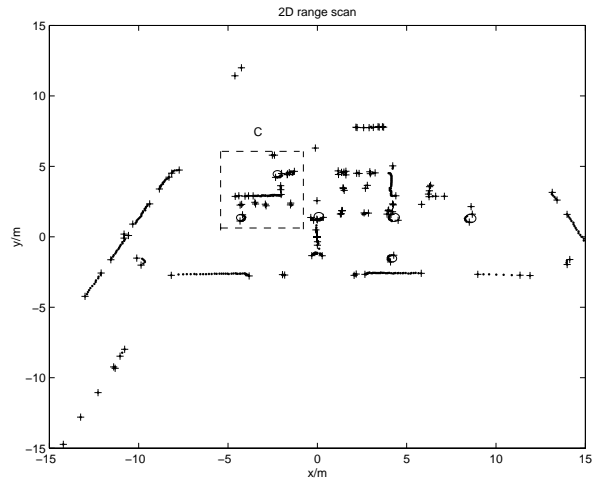
Fig. 3. Features extracted from data scanned at position 2.

presented which use circular features from trees. We calculate the relative errors of the estimated center coordinates and radius of each pillar as follows:

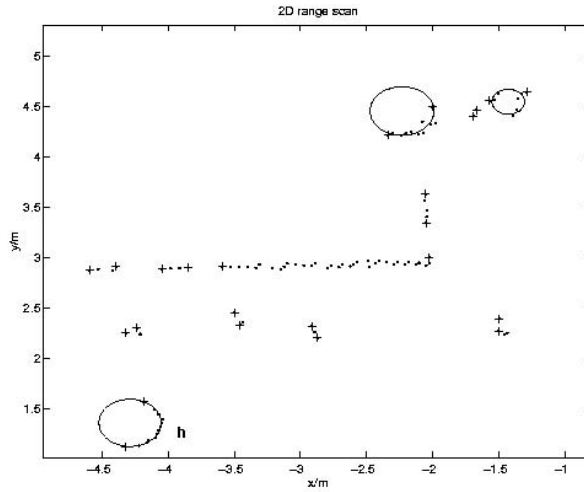
$$CE = \frac{\sqrt{(x_{true} - x_{estimate})^2 + (y_{true} - y_{estimate})^2}}{\sqrt{x_{true}^2 + y_{true}^2}} \quad (10)$$

$$RE = \frac{|r_{true} - r_{estimate}|}{r_{true}} \quad (11)$$

where x_{true} , y_{true} and r_{ture} are the actual coordinates and the actual center of the circle feature which are obtained from hand measurements and $x_{estimate}$, $y_{estimate}$ and $r_{estimate}$ are their estimated values. The results are shown



(a) Circles and edges extracted from data scanned at position 4 (the normal view).



(b) A zoomed view of the region inside box C in Fig. 4(a).

Fig. 4. The features extracted from data scanned at position 4.

in Tables 1 and 2.

Table 1

A comparison of the error CE of the four circular features between the proposed method and the method in [4]

	pillar d	pillar e	pillar f	pillar g
Proposed method	0.0179	0.0158	0.0136	0.0137
The method in [4]	0.0251	0.0244	0.0271	0.0166

Table 2

A comparison of the error RE of the four circular features between the proposed method and the method in [4]

	pillar d	pillar e	pillar f	pillar g
Proposed method	0.0373	0.0011	0.1057	0.0588
The method in [4]	0.2096	0.2326	0.2626	0.1384

From the above tables and the experiment carried out here, we can see that the proposed method can be more accurate than the method suggested in [4].

In order to test the feature extraction method for localization, two outdoor experiments have also been carried out on simultaneous localization and map building using the proposed feature extraction algorithm. The first experimental environment is shown in Figure 5(b). There are 8 tall trees and building walls and some bushes which constitute the semi-structured outdoor environment. For this semi-structured environment, the main features for localization are tree trunks. The proposed feature extraction algorithm is applied for extracting the features. The vehicle used in the experiment is Cycab, a car-like vehicle, as shown in Figure 5(a). It is equipped with a laser range sensor, Sick LMS 200, with dead reckoning capabilities. There are four wheel encoders. A DGPS with up to 2cm accuracy is used as a reference to give the ground truth of the vehicle pose to obtain the estimation error.

In the experimental environment, the vehicle moves along the path as shown in Figure 5(c) where the stars denote the trees of the environment which are detected, the dashed line indicates the real pose of the vehicle and the solid line means the estimated path using the simultaneous localization and mapping algorithm with the proposed feature extraction method. The data association method in the implementation is the same as that in [23]. Figure 5(d) shows a typical laser scan from this experiment. The dashed box A indicates the zoomed region shown in Figure 5(e). In these two figures, there are lines, arcs and edges (point features). However, in the experiment, we only use circle features from the tree trunks for localization. The 8 features are all detected during the SLAM process after the continuous observation, see Figure 5(c). It should be noted that there are false features that are detected in some scans, but they have not been used for the SLAM for more than 3 times. Hence, we did not draw them in the map. Here, the false features mean that the features which has not been confirmed as useful features during SLAM process.

To make a comparison on feature extraction performance, we also implement the method in [4]. Figure 6(a) shows the range and bearing innovations of the measurements when we apply the feature extraction method in [4] and our method during SLAM and their 3σ bounds. The dash-dot line in the middle of each sub-figure is the result of the localization using our proposed

feature detection method whereas the solid line in the middle is the result of the localization by the feature detection method in [4]. Figure 6(b) shows the vehicle’s position and orientation prediction errors and their 3σ error bounds. Further, we calculate the average absolute estimation error as defined by

$$\Delta x = \frac{\sum|\Delta x_i|}{N}; \quad \Delta y = \frac{\sum|\Delta y_i|}{N}; \quad \Delta\theta = \frac{\sum|\Delta\theta_i|}{N}$$

where Δx_i , Δy_i and $\Delta\theta_i$ are the vehicle pose errors at each time instant and N is the time step of the whole localization process. The comparison of the “average absolute error” for the two methods is given in Table 3.

Table 3

The errors $\Delta x, \Delta y, \Delta\theta$ of the vehicle pose when using different feature detection methods

	Proposed method	Method in [4]
Δx	0.0575	0.0823
Δy	0.0571	0.0732
$\Delta\theta$	0.0353	0.0528

In the table, the units for Δx and Δy are meters and that for $\Delta\theta$ is radians.

We also examine the false feature detection rate (the ratio of the number of false features to the total number of detected features in a scan) of the two algorithms. The maximum false detection rates for our algorithm and the method of [4] are respectively 0.125 and 0.111. And the average false detection rates are compared in Table 4.

Table 4

A comparison of the average false detection rate (20 scans) between the proposed method and the method in [4]

	scan 20 to 40	scan 60 to 80	scan 100 to 120	scan 140 to 160
Proposed method	0.027	0.031	0.029	0.033
The method in [4]	0.025	0.029	0.030	0.032

From the table, we know that the false detection rate of the method in [4] is a little lower than our method. We also note that the Bailey’s approach is more general in detecting irregular circular features. However, the false detection rates of both the algorithms are considered to be low.

It should be noted that there are false features that are detected in some scans, but they have not been used for the SLAM more than 3 times. Hence, we did not draw them in the map. Here, the false features mean those features which can not be confirmed as useful features (used for more than 3 times) for SLAM process.

The other testing site is a long pavement around Hall 7 at Nanyang Technological University. The real campus map including this pavement is shown in Fig. 7(a). Dead reckoning sensors and the sick laser range sensor are combined to predict the vehicle’s trajectory using the EKF and to build the map at the same time. During SLAM, in order to improve our map accuracy, we apply two types of features, namely point features (edges) and circular features, detected by the proposed method and the data association algorithm in [23].

For circular features, the proposed modified Gauss-Newton optimization method is applied to obtain their parameters. For a data group which has only 2 to 3 points, the average values of the x and y coordinates will be the parameters of the point feature. For predominant edge features, the parameters have been obtained during the data segmentation process. It should be noted that here a predominant edge feature means an edge which is far away from other edges. In our experiment, we set the Euclidean distance to be 5 meters.

Fig. 7(b) shows the part of our experimental environment. Figure 8(a) gives a typical laser scan during the process. Figure 8(b) shows the circle features extracted from a laser scan for the region inside Block E of Figure 8(a). Since the environment involves a large number of edges in some places, we only use those predominant edges on one side of the road according to the angles between the extracted features and the robot. We also limit the distance (no more than 15 meters) from the features and the sensor to deduce the number of features. During SLAM, in order to reduce the number of noisy edges, we adopt the strategy—if an edge feature is not observed in 10 successive scans, we consider it out-of-dated and remove it from the map. Tentative features that are not re-observed for more than 3 times are also removed from the map after a fixed time interval has elapsed.

Fig. 8(c) shows the results of SLAM. We can see that the estimated path is very close to the DGPS estimated path (considered to be ground truth here). In this figure, there is a break in the DGPS data. This is because the vehicle is under a building to make a turn where the DGPS signal is blocked. The average position error of the entire SLAM process except the segment where the ground truth is unavailable is smaller than 0.5 meters. The features’ map is also shown in this figure (those denoted by stars). It is noted that the features’ map is constituted by those features that are extracted and used during SLAM more than 3 times. Figures 8(d) and 8(e) indicate the observation innovations and their 2σ confidence bounds during the whole process.

Remark 3.1 *The second experimental results are not as good as we expected. Some new research work which can improve SLAM process including feature extraction is still needed in the future.*

4 Conclusions

In this paper a new algorithm for feature detection in semi-structured outdoor environments has been presented. It can be used for the extraction of planar surfaces, tree trunks or tree-like objects and edges in semi-structured outdoor environments for mobile robot navigation. Experimental results show that the proposed method can extract features for navigation purposes successfully.

References

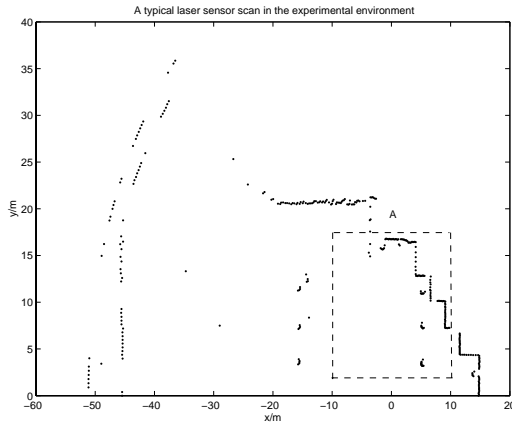
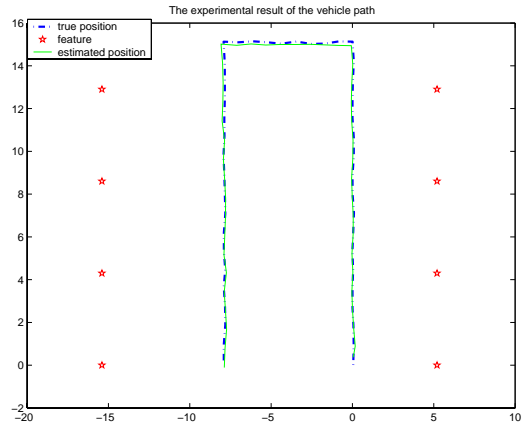
- [1] M. D. Adams, S. Zhang, and L. Xie, Particle filter based outdoor robot localization using natural features extracted from a laser scanner, in *Proc. of IEEE Int. Conf. Robot. Automat.*, New Orleans, USA, April 2004, pp. 854–859.
- [2] M. D. Adams, Sensor modelling, Design and Data Processing for Autonomous Navigation. World Scientific, 1999.
- [3] M. D. Adams and A. Kerstens, Tracking naturally occurring indoor features in 2D and 3D with lidar range/amplitude data, *The International Journal of Robotics Research*, 17 (1998) 907-923.
- [4] T. Bailey, Mobile robot localization and mapping in extensive outdoor environments, University of Sydney Ph.D Thesis, 2002.
- [5] J. L. Crowley, Navigation of an intelligent mobile robot, *IEEE Journal of Robot Automation*, RA-1 No.1 (1985) 31-41.
- [6] J. E. Dennis and R. B. Schnabel, Numerical Methods for Unconstrained Optimization and Nonlinear Equations. Prentice-Hall, 1983.
- [7] G. Dissanayake, P. Newman, S. Clark, H. F. Durrant-Whyte and M. Csorba, A solution to the simultaneous localization and map building (SLAM) problem, *IEEE Transactions on Robotics and Automation* 17 (2001) 229-241.
- [8] D. Dori and W. Liu, Stepwise recovery of arc segmentation in complex line environments, *International Journal on Document Analysis and Recognition*, 1(1998):62-71.
- [9] P. Dosch, G. Masini, and K. Tombre, Improving arc detection in graphics recognition, in: *Proceedings of the International Conference on Pattern Recognition*, Barcelona, Spain, 2000, pp. 243-246.
- [10] J. E. Guivant, F. R. Masson and E. M. Nebot, Simultaneous localization and map building using natural features and absolute information, *Robotics and Autonomous Systems*, 40 (2002) 79-90.
- [11] J. E. Guivant, E. M. Nebot, and S. Baiker, Localization and map building using laser range sensors in outdoor applications, *Journal of Robotic Systems*, 17 (2000) 565-583.

- [12] F. Gustafsson, F. Gunnarsson, N. Bergman, U. Forssell, J. Jansson, R. Kalsson, and P. J. Nordlund, Particle filters for positioning, navigation, and tracking, *IEEE Transactions on Signal Processing*, 50 (2002) 425-436.
- [13] L. Iocchi and D. Nardi, Hough localization for mobile robots in polygonal environments, *Robotics and Autonomous Syst.*, 40 (2002), 43-58
- [14] S. Julier, J. Uhlmann, and H. F. Durrant-Whyte, A new method for the nonlinear transformation of means and covariances in filters and estimators, *IEEE Transactions on Automatic Control* 45 (2000) 477-482.
- [15] J. J. Leonard and H. F. Durrant-Whyte, Application of multi-target tracking to sonar based mobile robot navigation, in: *Proceedings of the IEEE International Conference on Decision Control*, Chicago, USA, 1990, pp. 3118-3123.
- [16] J. Nocedal and S. J. Wright, *Numerical Optimization*, Springer Verlag, 1999.
- [17] S. I. Roumeliotis and G. A. Bekey, Segments: a layered, dual Kalman filter algorithm for indoor feature extraction, in: *Proceedings of IEEE/RSJ International Conference on Intelligent Robots and Systems*, Japan, 2000, pp. 454-461.
- [18] R. M. Taylor and P. J. Probert, Range finding and feature extraction by segmentation of images for mobile robot navigation, in: *Proceedings of the IEEE International Conference on Robotics and Automation*, Minnesota, USA, 1996, pp. 95-100.
- [19] J. Vandorpe, H. Van. Brussel and H. Xu, Exact dynamic map building for a mobile robot using geometrical primitives produced by a 2D range finder, in: *Proceedings of the IEEE International Conference on Robotics and Automation*, Minnesota, USA, 1996, pp. 901-908.
- [20] S. B. Williams, Efficient solutions to autonomous mapping and navigation problems, *Universsity of Sydney Ph.D Thesis*, 2001.
- [21] S. Zhang, L. Xie, and M. D. Adams, An Efficient Data Association Approach to Simultaneous Localization and Map Building, *The International Journal of Robotics Research* 24 (2005) 49-60.
- [22] S. Zhang, L. Xie, and M. D. Adams, Geometrical feature extraction using 2d range scanner, in *Proc. of the Fourth Int. Conf. Contr. and Automat.* , Montreal, Canada, June 2003, pp. 901-905.
- [23] S. Zhang, L. Xie, and M. D. Adams, An Efficient Data Association Approach to Simultaneous Localization and Map Building, in *Proc. of IEEE Int. Conf. Robot. Automat.*, New Orleans, USA, April 2004, pp. 1493-1498.
- [24] S. Zhang, L. Xie, and M. D. Adams, Gradient model based feature extraction for simultaneous localization and mapping in outdoor applications, *Proceedings of the Eighth International Conference on Control, Automation, Robotics and Vision (ICARCV 2004)*., Kunming, China, December 2004, pp.431-436.



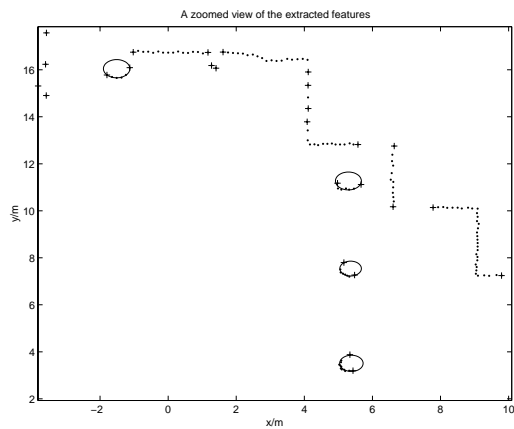
(a) The Cycab, a car-like vehicle used in the experiment.

(b) The first SLAM experimental environment (the whole scene).



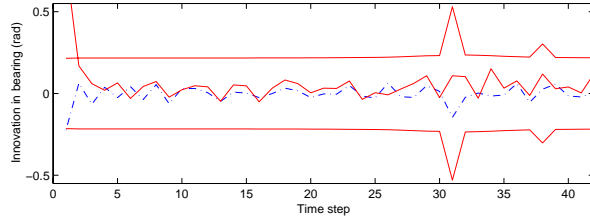
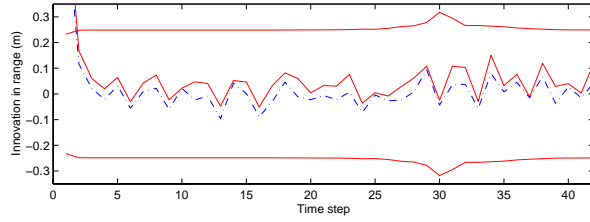
(c) The estimated path and the true trajectory of the vehicle during the SLAM of the first SLAM experimental environment.

(d) A complete 180 degree scan data corresponding to figure 5(b).

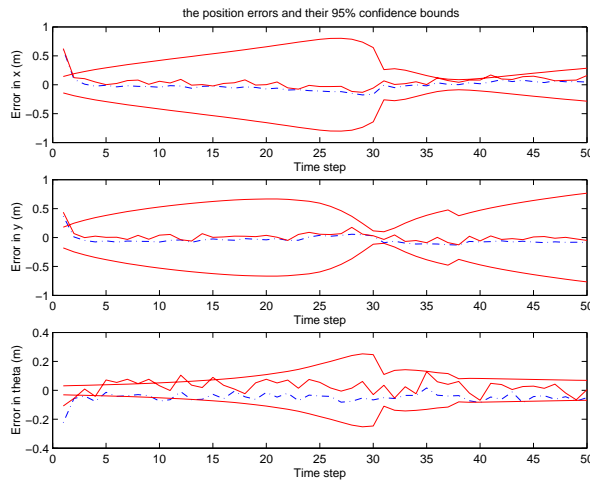


(e) The circular features (trees) and edges extracted from the environment in figure 5(b) using the Gauss-Newton algorithm.

Fig. 5. The vehicle, environment and SLAM results from the proposed feature detection method.



(a) A comparison on range and bearing innovations during localization when using the proposed method (dash-dot line) and the method in [4] (solid line in the middle).



(b) The error and 3σ error bounds of the vehicle when using different feature detection methods. The dashed line is the result of localization using the proposed feature detection methods.

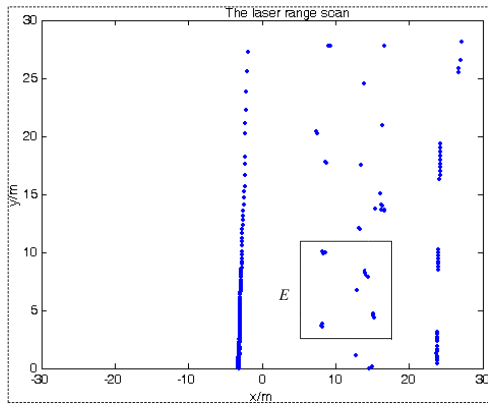
Fig. 6. A comparison of localization results by using the proposed method and another published method.



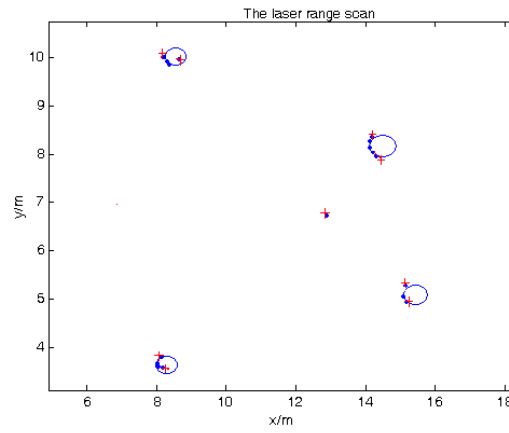
(a) The map of our site.

(b) The environment and the vehicle used in the experiments.

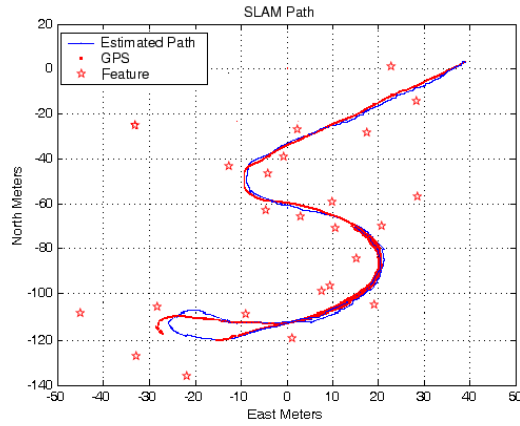
Fig. 7. The feature extraction and SLAM experiments.



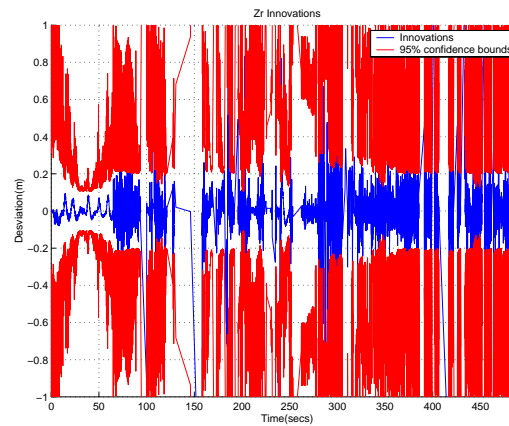
(a) A typical laser scan during the vehicle moving.



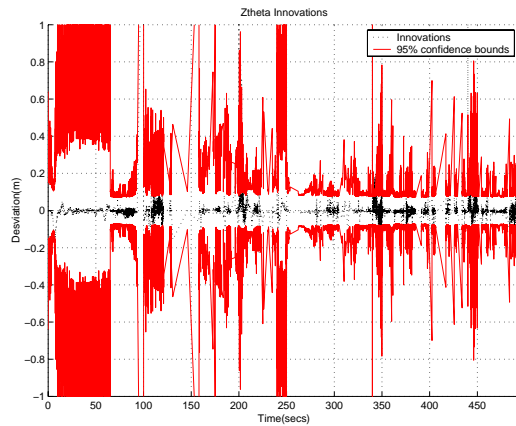
(b) The features (circular features and edges) extracted from the zoomed view of the block E in Fig. 8(a).



(c) The features' map and the comparison of the estimated path and GPS readings of the path during SLAM.



(d) The range observation's innovation and their 95% confidence bounds in our SLAM experiment.



(e) The angular observation innovations and their 95% confidence bounds in the SLAM experiment.

Fig. 8. SLAM results using the proposed feature detection method.